Electronic Supporting Information

for

Cellulose Nanocrystal Gels as Radical Reservoirs

Jiaou Ren,[a] Yota Neagari,[a] Yihan Shi,[a] Zongzhe Li,[a] Lucas J. Andrew,[a] Miguel A. Soto,[a,b*] and Mark J. MacLachlan[a,c,d*]

[a] Department of Chemistry, University of British Columbia, 2036 Main Mall, Vancouver, British Columbia V6T 1Z1, Canada

[b] Department of Chemistry, University of Saskatchewan, 110 Science Place, Saskatoon, Saskatchewan S7N 5C9, Canada

[c] Quantum Matter Institute, University of British Columbia, 2355 East Mall, Vancouver, BC, V6T 1Z4 Canada

[d] WPI Nano Life Science Institute, Kanazawa University, Kanazawa, 920-1192 Japan

Table of Contents

1. Materials and methods

Cellulose nanocrystal suspensions (CNCs) were provided by FPInnovations (5.0 wt%, pH 5.3, ζ = -60 mV) and stored at 4 °C. All precursors used in syntheses were purchased from Sigma-Aldrich and used without further purification. ITO glass (thickness: 1.10 ± 0.05 mm; resistance/sq: 10–15 Ω; transmittance: ≥85%) was purchased from Adafruit. UV-vis spectra were recorded on an Agilent, Cary 5000 UV-vis-NIR spectrophotometer, using quartz cuvettes with 1.0 cm pathlengths. For measurements under applied voltage, the UV-vis spectrometer was coupled to either a bipotentiostat model AFCBP1 (Pine Instrument Company) or a direct-current (DC) power supply (LX 60-1, XANTREX). For electrochromic devices, fully assembled cells (consisting of gels sandwiched between two ITO glass substrates) were taped directly onto a solid sample holder with a circular aperture (1 mm in diameter). Background correction was performed using an empty sample holder. Spectra were collected over the wavelength range of 200–800 nm with a step size of 1 nm. Cyclic voltammetry measurements were conducted using a bipotentiostat model AFCBP1 (Pine Instrument Company) at a scan rate of 100 mV/s. A two-electrode system was employed for electrochromic devices assembled in a sandwich configuration with ITO glass serving as both the working and counter electrodes (WE, CE).

Rheology measurements were conducted using an Anton Paar MCR 502 rotational rheometer. Zeta-potential measurements were conducted in an Omni Nanobrook Analyzer from Brookhaven Instruments Corporation, using PALS (phase analysis light scattering) mode. Photoirradiation experiments were performed inside a chamber, using a UV lamp equipped with two 302 nm fluorescent tubes (8 W, 0.32 amp), all samples were located at ~ 10 cm from the light source when photoirradiated.

Color development of the photoconverted material under sunlight was recorded as a video. The video was segmented into individual frames, and each frame was converted to grayscale intensity values using ImageJ. These values were then used to calculate the fractional color development (α) according to:

$$\alpha = \frac{I_0 - I_t}{I_0 - I_f}$$

where $I_0$is the initial grayscale intensity of the material, $I_t$is the intensity at time t, and $I_f$is the final intensity after complete color development.

Viologens **1**,[1] **3**,[2] and **5**[3] were synthesized following reported methodologies. ^{1}H NMR characterization data matched those reported in the literature.

2. Materials synthesis

2.1 Gelator solutions

The deep eutectic solvent (DES) was prepared by heating glycerol (46 g, 0.50 mol) and choline chloride (35 g, 0.25 mol) at 80 °C with stirring for 30 min. Stock solutions of compounds **1** (50 mM), **3** (25 mM) and, **5** (25 mM) were prepared in DES at 80 °C. All stock solutions and DES were cooled down to room temperature prior to gel synthesis.

2.1 Gels

General method. The corresponding gelator (DES, DES–**1**, DES–**3**, DES–**5**, or DES–**1**/**5**) was mixed with aqueous CNCs (5 wt%, pH = 5.3), in the ratios listed in Tables S1–S3, and mixed using a vortex mixer (3200 rpm, 1 min). All gels were stored in the dark at room temperature until further use. For solvent exchange (water to DES), the corresponding gel was immersed in DES (15 mL) for 8 h, the supernatant was removed and replaced with fresh DES (25 mL). The process was repeated for a total of three times. The gel was removed from DES and stored in a sealed vial away from ambient light.

CNC–DES. Gels were prepared as shown in Table S1, using DES as the gelator.

Table S1. CNC and DES content in CNC–DES gels.

Aqueous CNCs (μl)	**DES** (μL)	**[Gelator]** (vol%)
1987	13	0.63
1975	25	1.25
1950	50	2.5
1925	75	3.75
1900	100	5.0
1850	150	7.5
1800	200	10

*CNC–**1***. Gels were prepared as shown in Table S2, using a stock solution of **1** in DES as the gelator.

Table S2. CNC and **1** content in CNC–**1** gels.

Aqueous CNCs (μl)	**1 (μL)**	**[Gelator]** (vol%)	**[1]** (mM)
1987	13	0.63	0.32
1975	25	1.25	0.63
1950	50	2.5	1.25
1925	75	3.75	1.88
1900	100	5.0	2.50
1850	150	7.5	3.75
1800	200	10	5.00

*CNC–**3***. Gels were prepared as shown in Table S3, using a stock solution of the corresponding viologens in DES.

Table S3. CNC and gelator content in gels CNC–DES–**3**, CNC–DES–**5** and or CNC–DES–**1**/**5**.

Aqueous CNCs (μl)	**Gelator**	**Gelator volume**	**[Gelator]** (vol%)	**[viologen]** (mM)
1800	DES–**3**	200	10	2.5
1800	DES–**5**	200	10	2.5
1700	DES–**1**/**5**	100 (**1**) 200 (**5**)	5 (**1**) 10 (**5**)	2.5 (**1**) 2.5 (**5**)

3. Characterization

3.1 CNC–DES gels

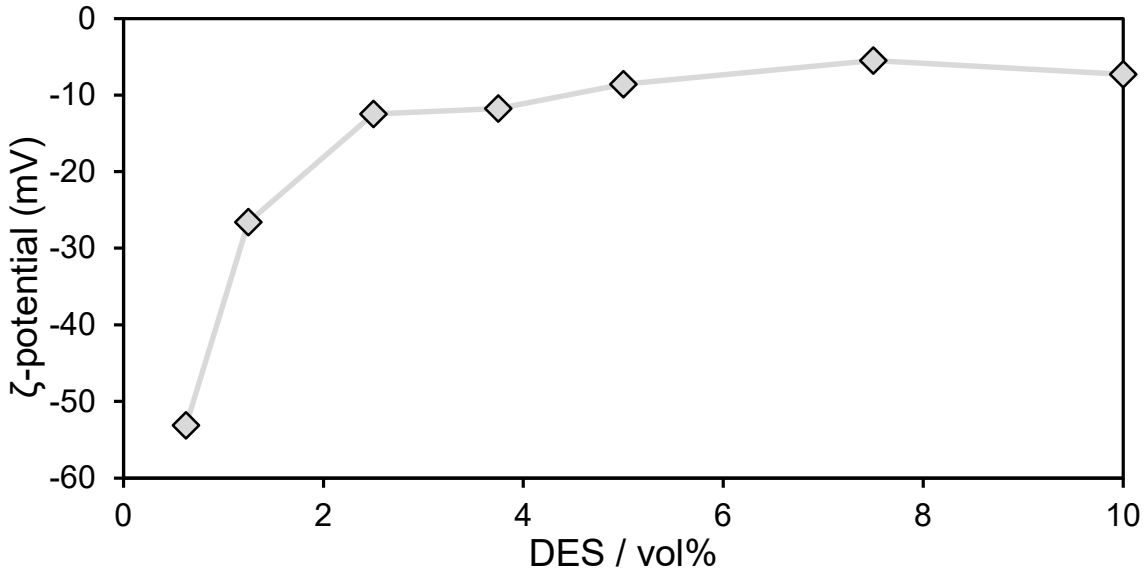

Figure S1. ζ-Potential of CNC–DES gels prepared with varying concentrations of DES, as shown in Table S1.

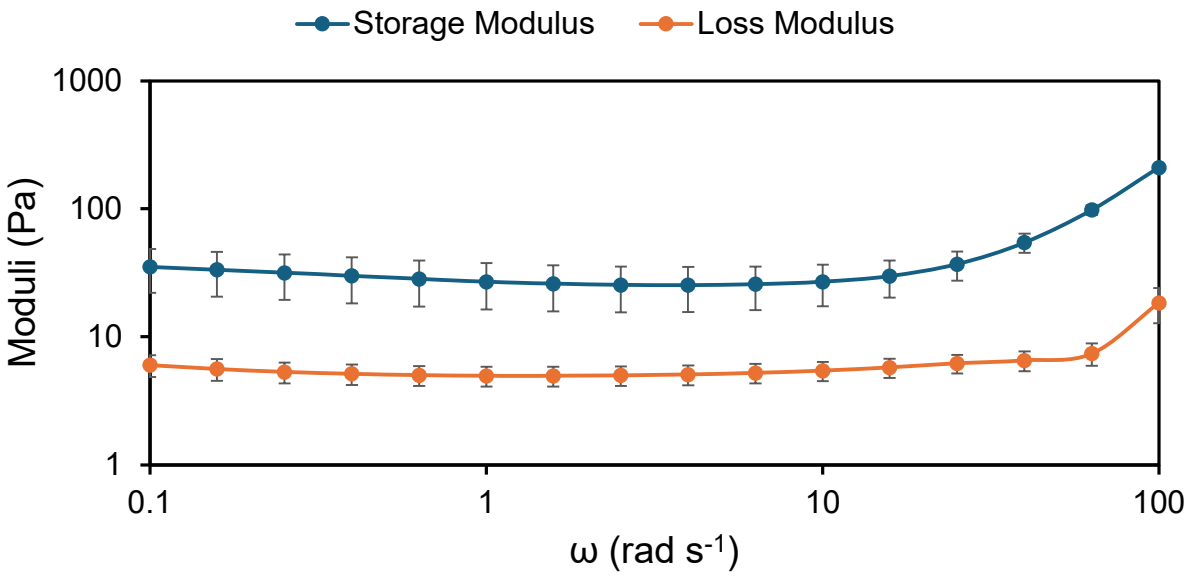

Figure S2. Storage and loss moduli of CNC–DES gel, [DES] = 1.25 vol%. Error bars represent standard deviations from three independent measurements.

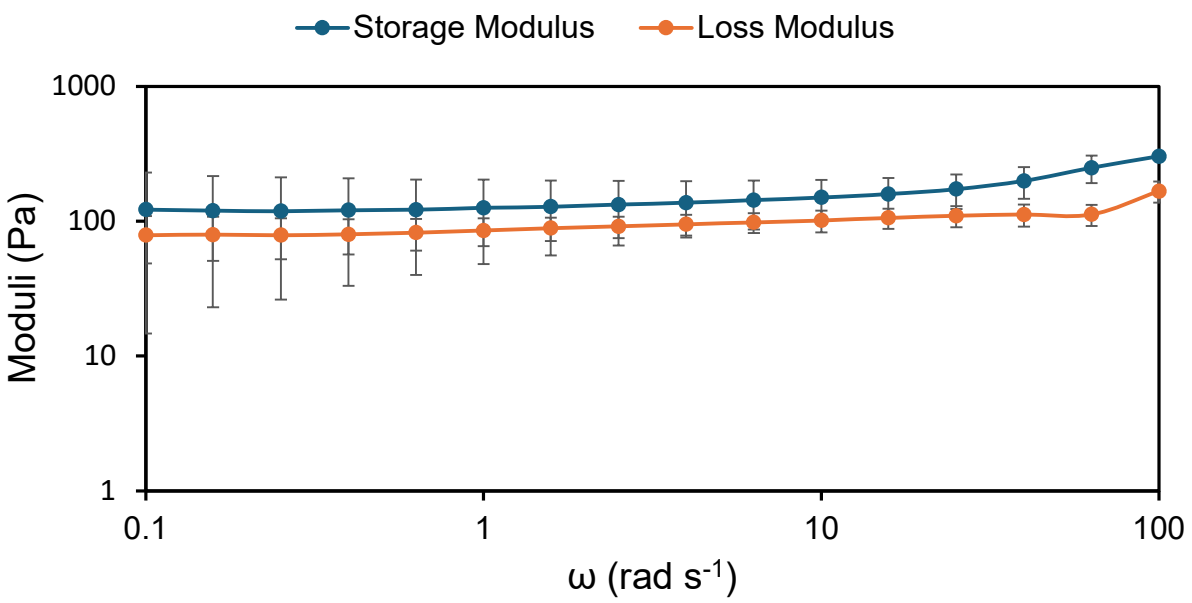

Figure S3. Storage and loss moduli of CNC–DES gel, [DES] = 2.5 vol%. Error bars represent standard deviations from three independent measurements.

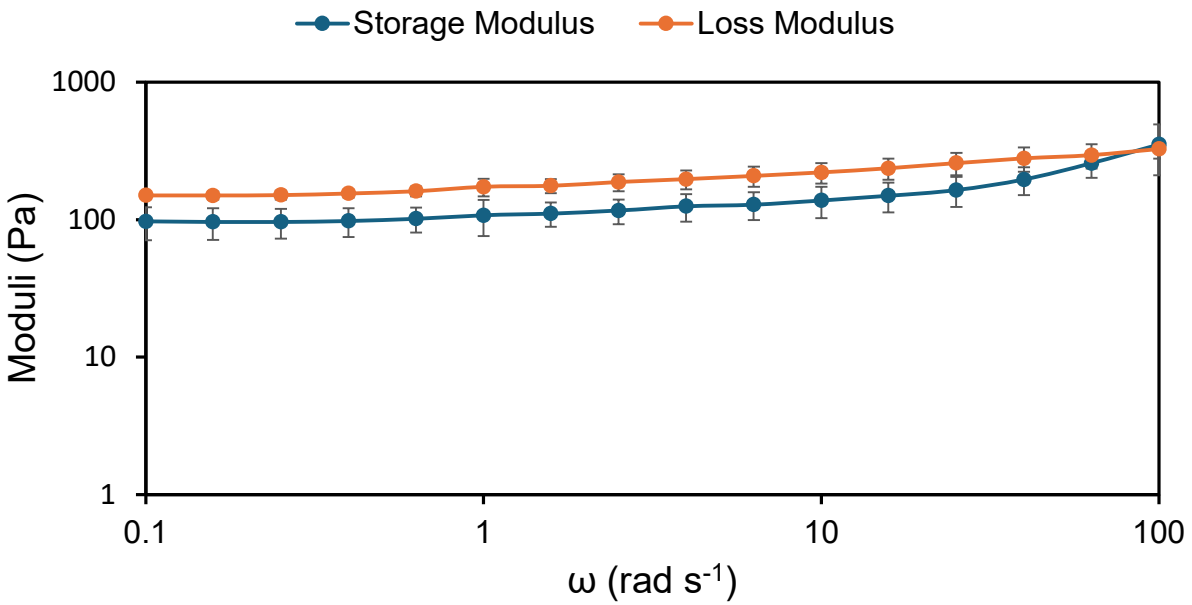

Figure S4. Storage and loss moduli of CNC–DES gel, [DES] = 5 vol%. Error bars represent standard deviations from three independent measurements.

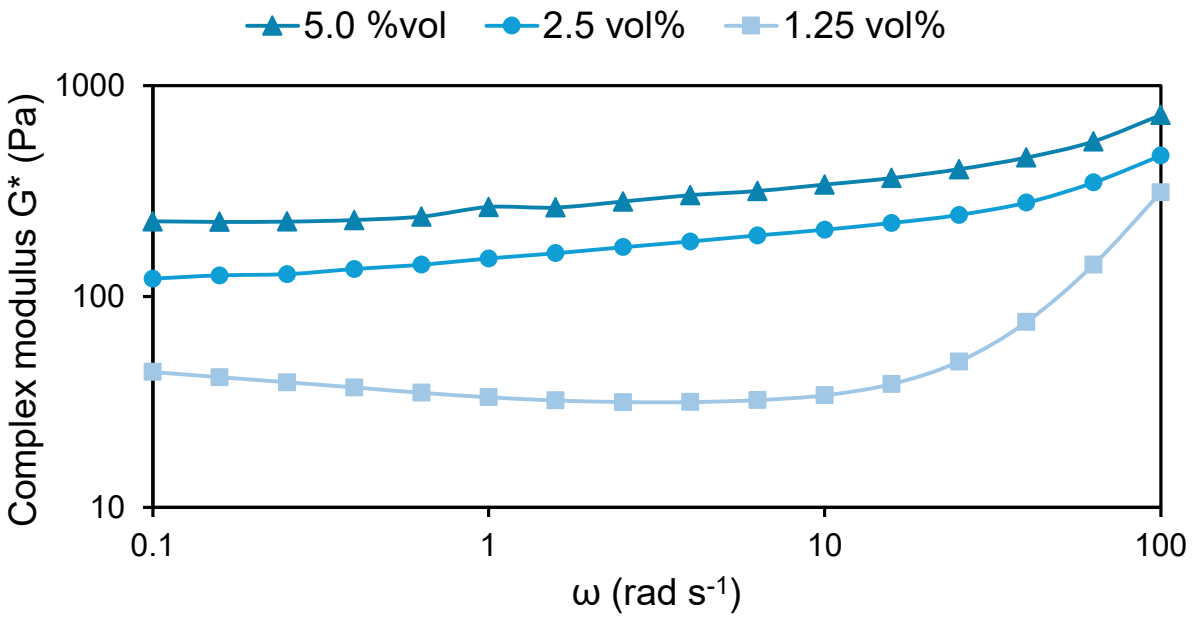

Figure S5. G* values of CNC–DES gels prepared with varying concentrations of DES.

3.2 CNC–1 gels

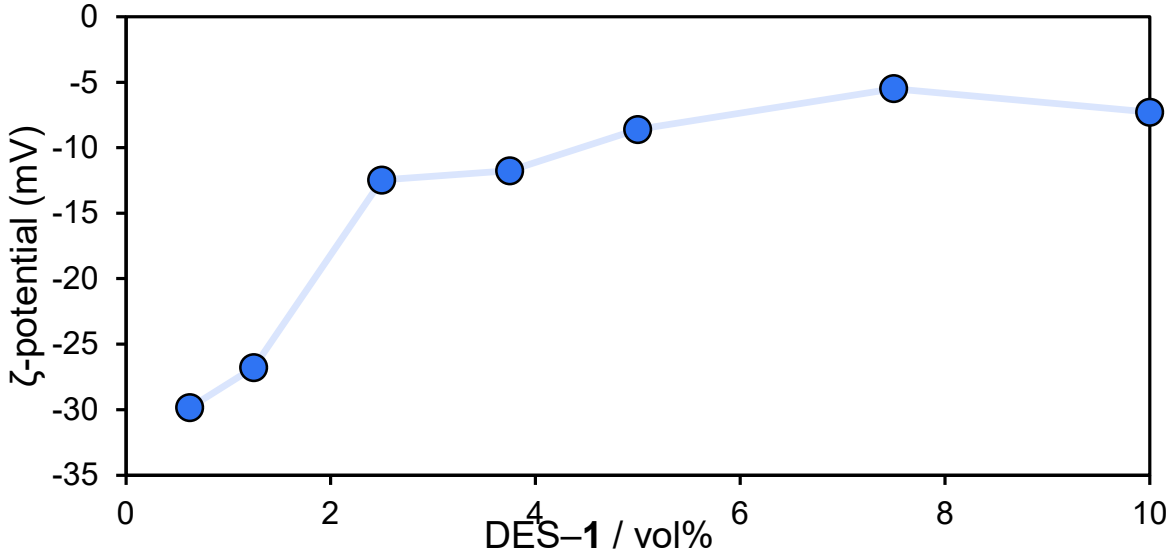

Figure S6. ζ-Potential of CNC–**1** gels prepared with varying concentrations of DES-**1**, as shown in Table S2.

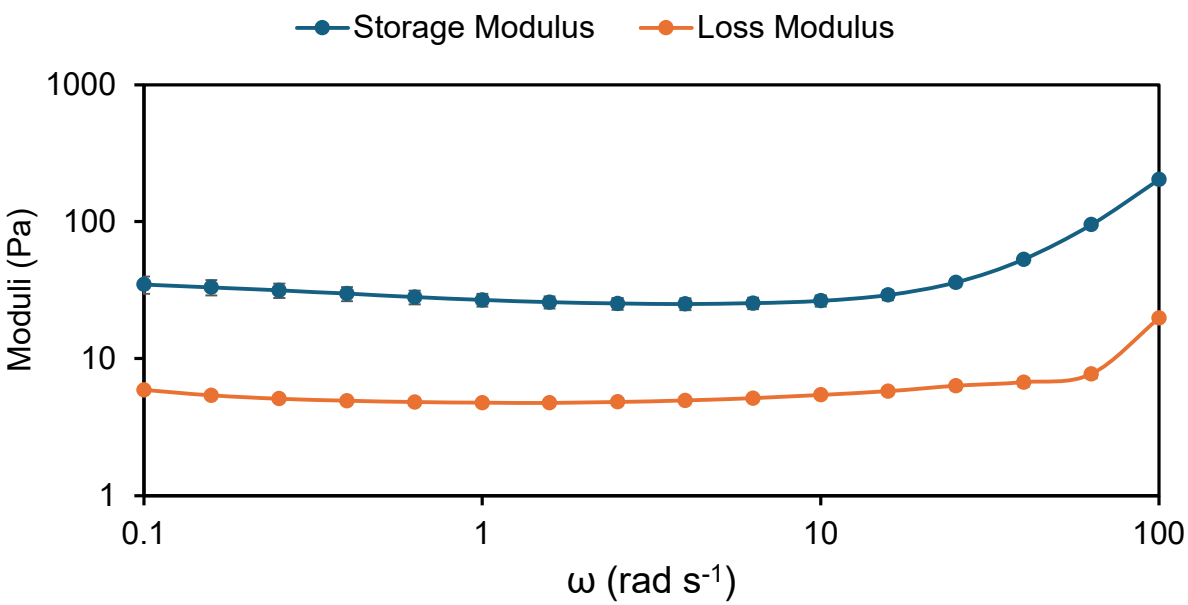

Figure S7. Storage and loss moduli of CNC–**1** gel, [DES–**1**] = 0.63 vol%. Error bars represent standard deviations from three independent measurements.

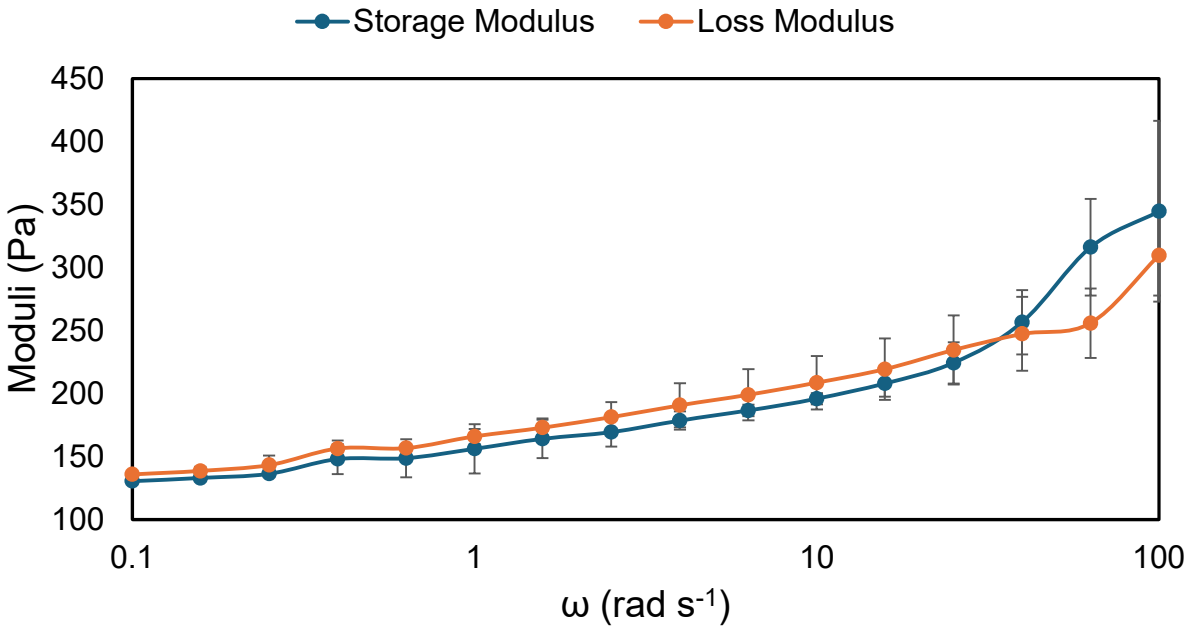

Figure S8. Storage and loss moduli of CNC–**1** gel, [DES–**1**] = 0.25 vol%. Error bars represent standard deviations from three independent measurements.

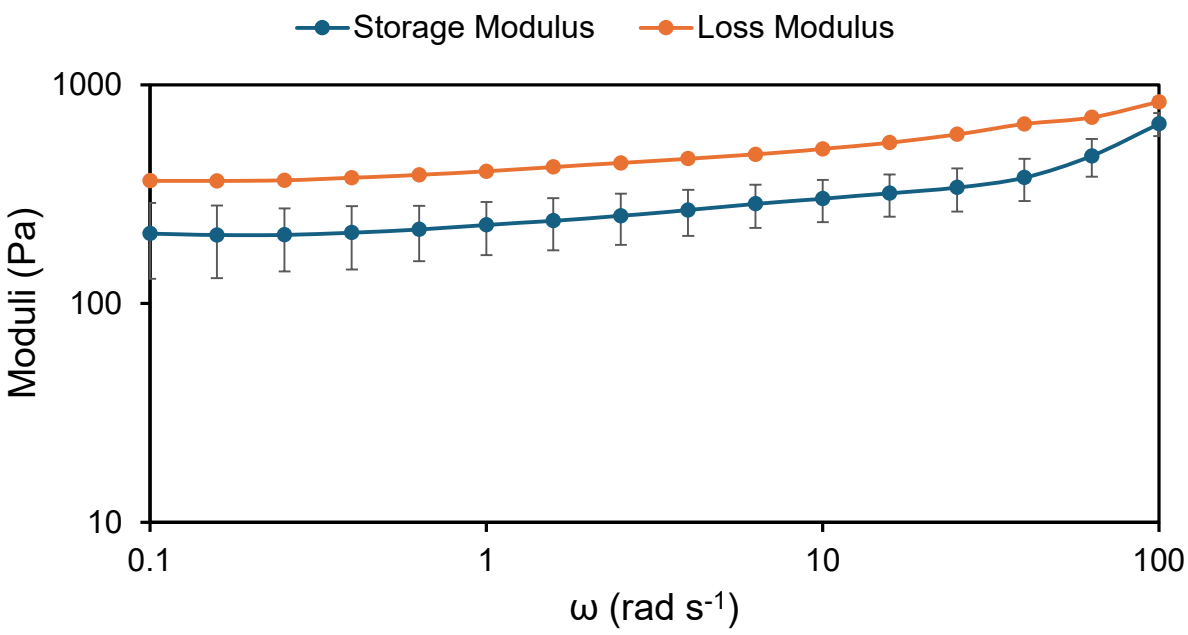

Figure S9. Storage and loss moduli of CNC–**1** gel, [DES–**1**] = 5 vol%. Error bars represent standard deviations from three independent measurements.

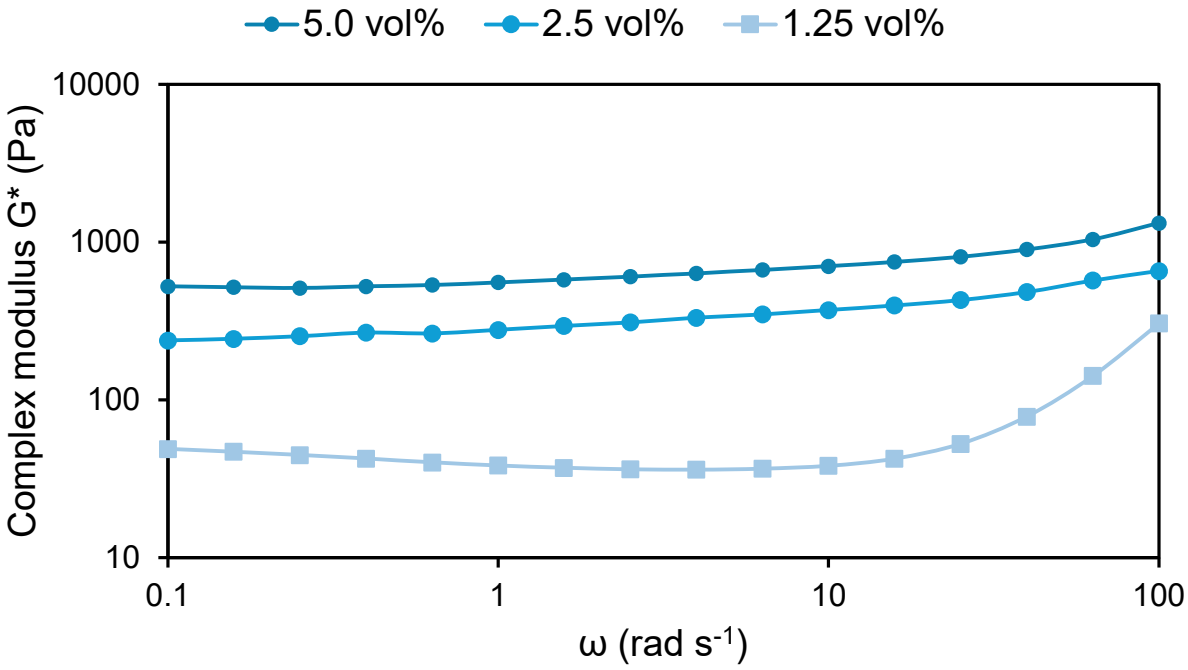

Figure S10. Complex modulus (G*) values of CNC–DES gels prepared with varying concentrations of DES–**1**.

3.3 CNC–DES–1 gels

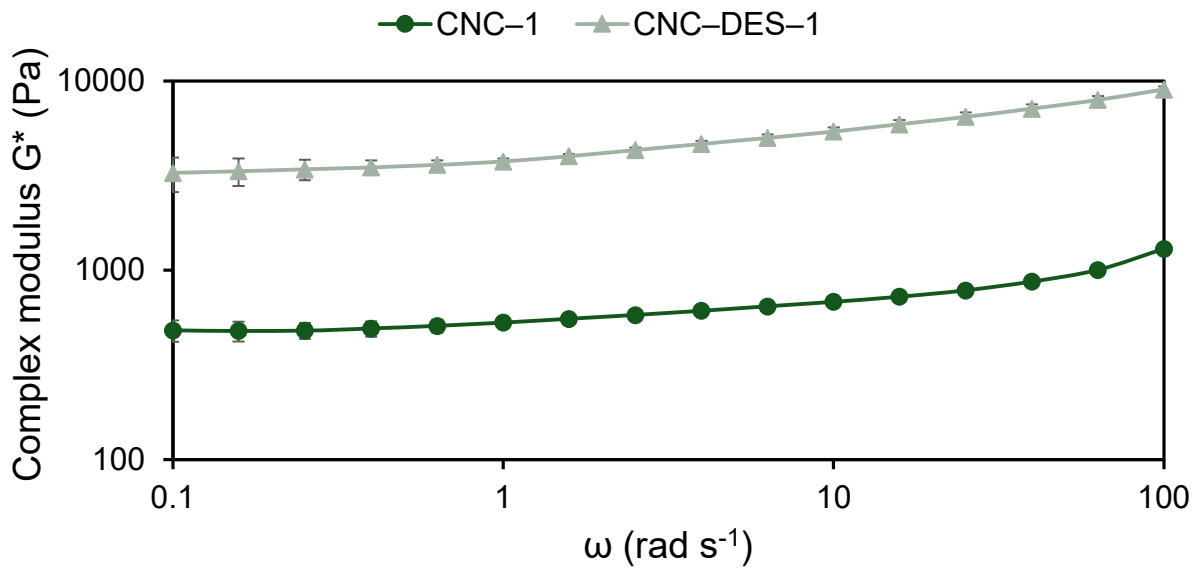

Figure S11. G* for CNC–**1** gels (prior to solvent exchange; water to DES) and CNC–DES–**1** (after solvent exchange). Error bars represent standard deviations from three independent measurements.

3.3 CNC–DES–2 gels

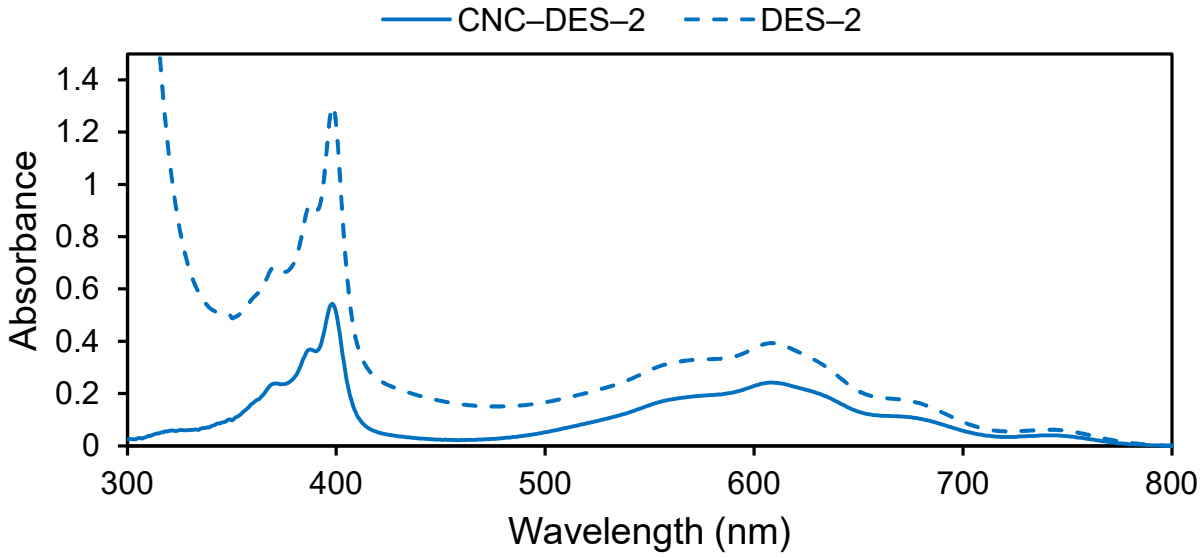

Figure S12. UV-vis spectra of CNC–DES–**2** gel and DES–2. A CNC–DES–**1** gel was prepared at 1.25 vol% of gelator, as shown in Table S2; the material was irradiated at 302 nm for 10 min to generate CNC–DES–**2** (continuous line). A 0.5 mM solution of **1** in DES was irradiated for 10 min to produce DES–**2** and analyzed by UV-vis spectroscopy (dashed line).

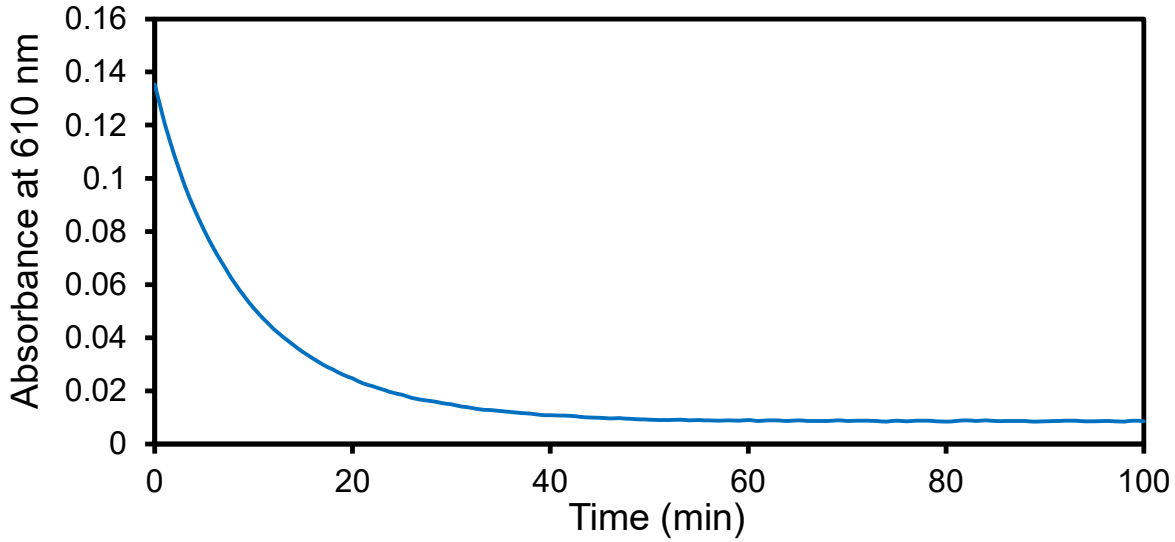

Figure S13. Time-dependant absorbance decay. Sample prepared at 1.25 vol% of gelator (**1**). The gel was spread onto the wall of a quartz UV-vis cuvette (~ 2 mm thick) and irradiated for 5 min at 302 nm. Absorbance was measured at 610 nm at a rate of 1 scan/min.

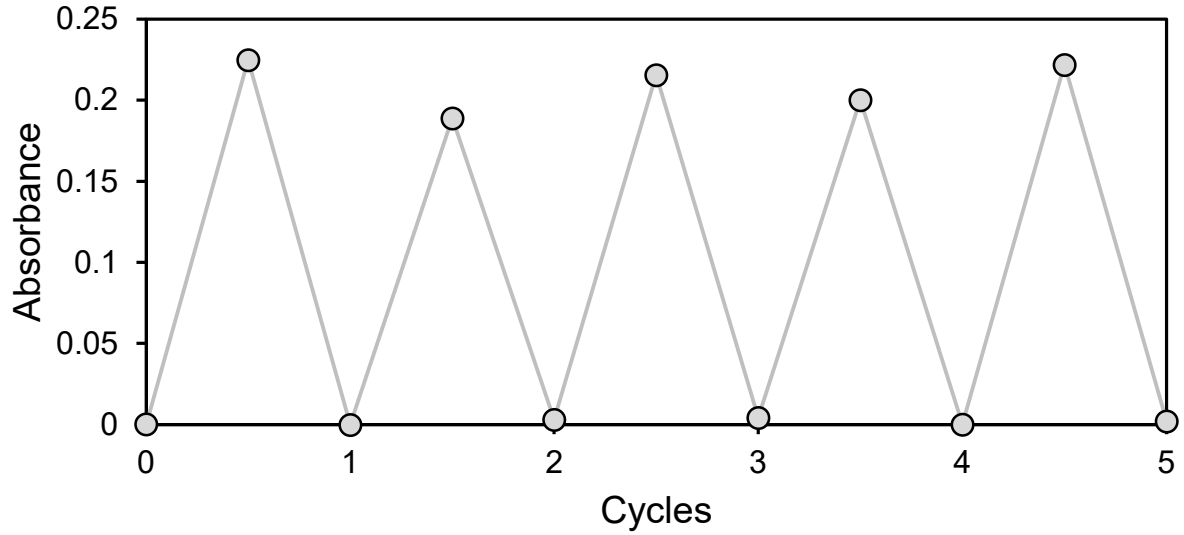

Figure S14. UV-vis Absorbance of gel upon multiple UV-recovery cycles (monitored at 575 nm).

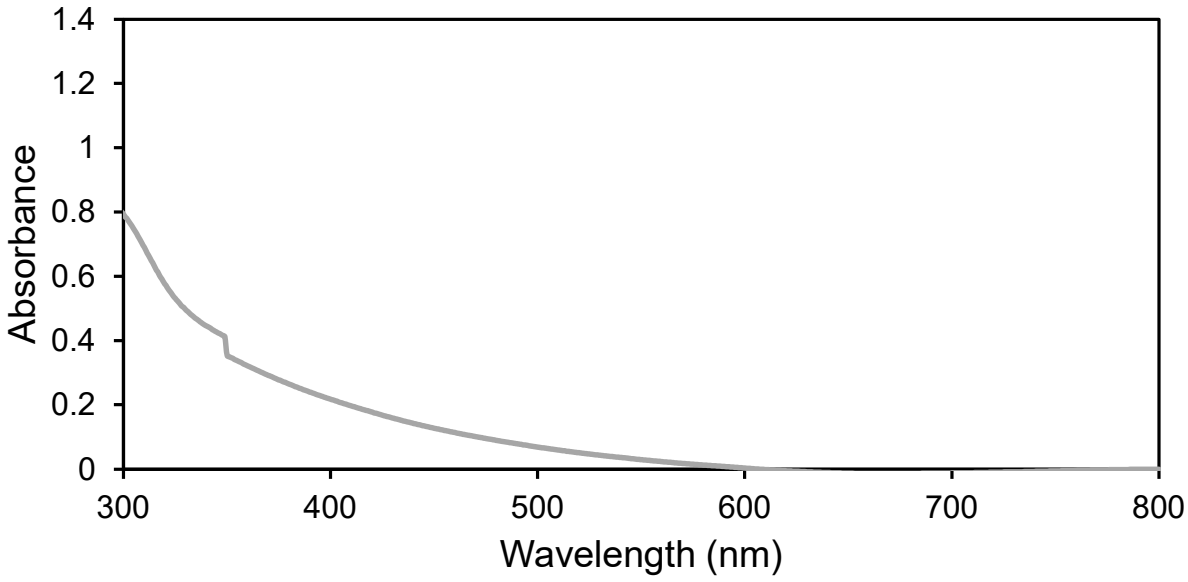

Figure S15. UV-vis spectrum of a CNC–DES–**1** gel after undergoing five cycles of photoreduction and oxidation. This represents the last point of the cycles shown in Figure S13.

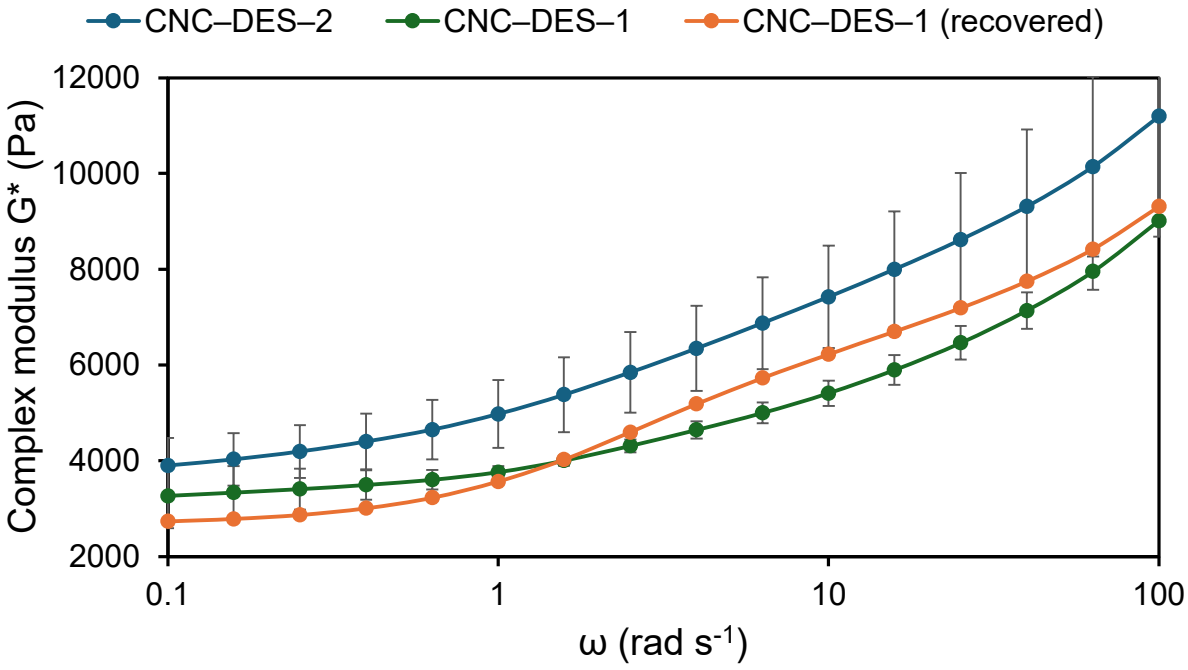

Figure S16. G* values of paraquat-containing gels before photoirradiation (CNC–DES–**1**), after irradiation (CNC–DES–**2**), and after full recovery (CNC–DES–**1**).

4. Electroactive materials

4.1 Fabrication of electrochromic devices

The electrochromic devices were fabricated in a sandwich-type assembly, as schematically illustrated in Figure S16. ITO glass substrates were cleaned sequentially with deionized water, acetone, and methanol. A double layer parafilm spacer (area: 12 × 12 mm^2, total thickness: 0.26 mm) was placed between two ITO glass plates to define the chamber volume (37 mm^3), which was then filled with CNC–DES–**1** or CNC–DES–**3** gels. The assembly was clamped to prevent leakage.

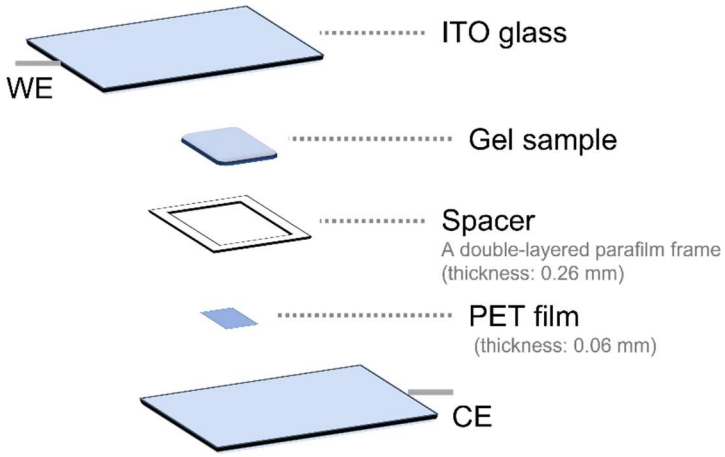

Figure S17. Schematic illustration of the device setup.

A two-electrode configuration was employed: the ITO glass plate in direct contact with the gel served as the working electrode (WE), and the opposite ITO glass plate served as the counter electrode (CE). For devices with CNC–DES–**1** gels, no PET film was applied.

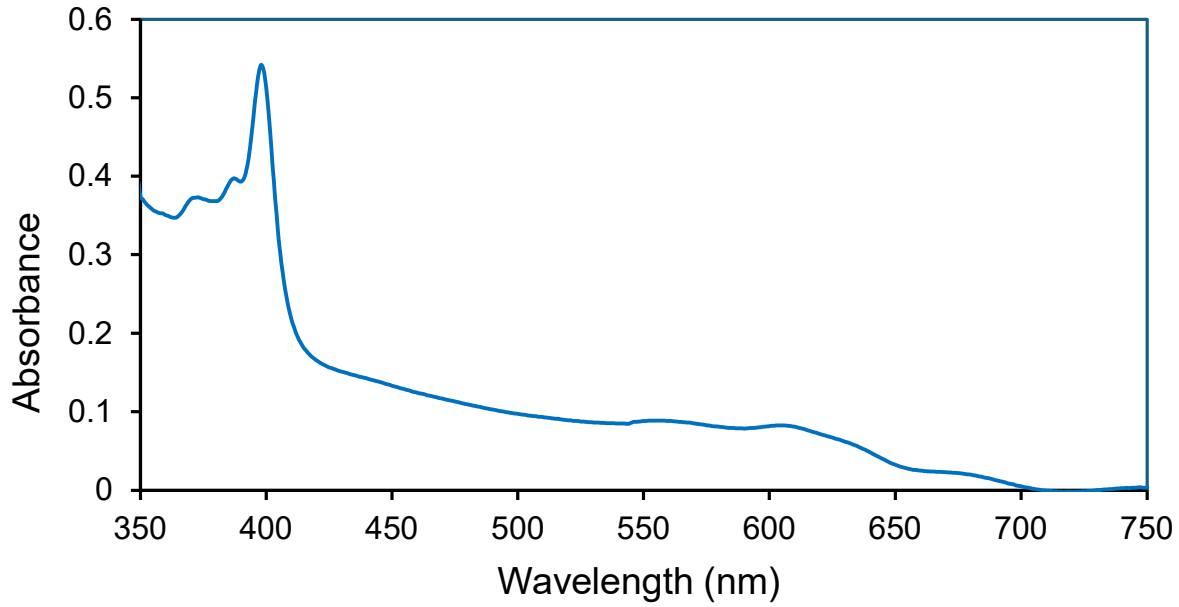

Figure S18. UV-vis Spectrum of CNC–DES–**1** after reduction at -2.5 V in the electrochromic devices**.**

4.2 Cycling stability

The cycling stability of the electrochromic devices was evaluated by a single-wavelength spectrophotometry method (604 nm for CNC–DES–**1**) using a UV-vis spectrophotometer coupled with a bipotentiostat model AFCBP1 (Pine Instrument Company). Measurements were carried out in transmission mode at room temperature under ambient atmosphere. Fully assembled devices, consisting of gels sandwiched between two ITO glass substrates, were taped directly onto a solid sample holder with a circular aperture (1 mm in diameter). Background correction was performed using an empty sample holder, which was defined as 100% transmittance (T).

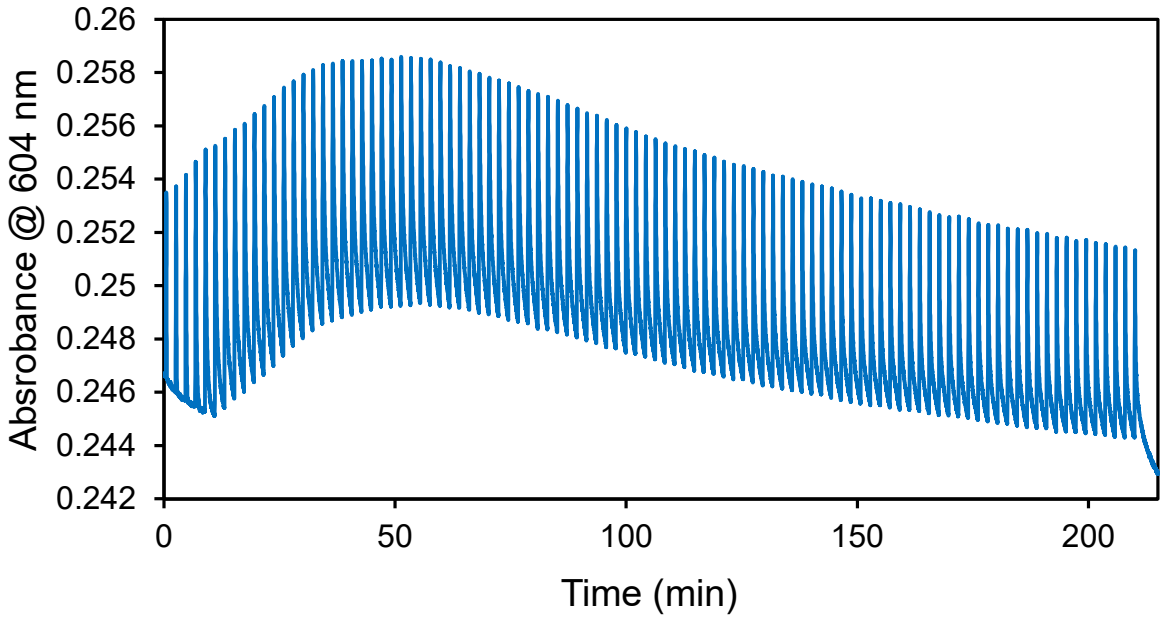

Figure S19. Gel UV-vis absorbance at 604 nm, with switching voltage in the electrochromic device.

4.3 Multicolor hidden text device

The multicolor hidden text device was fabricated in a sandwich-type assembly, as schematically illustrated in Figure S19. A double layer parafilm spacer (area: 12 × 36 mm^2, total thickness: 0.26 mm) was placed between two ITO glass plates to define the chamber volume (112 mm3), which was then filled with CNC–DES–**1** and CNC–DES–**3** gels. The device was secured with clips. A PET stencil mask with the "UBC" pattern was attached to one ITO surface to enable spatially controlled coloration of the gels under applied potential. Patterned coloration was recorded by applying a potential of –2.5 to –3.0 V for approximately 20 min (Video S2). The video was accelerated 15-fold to better visualize the coloration process.

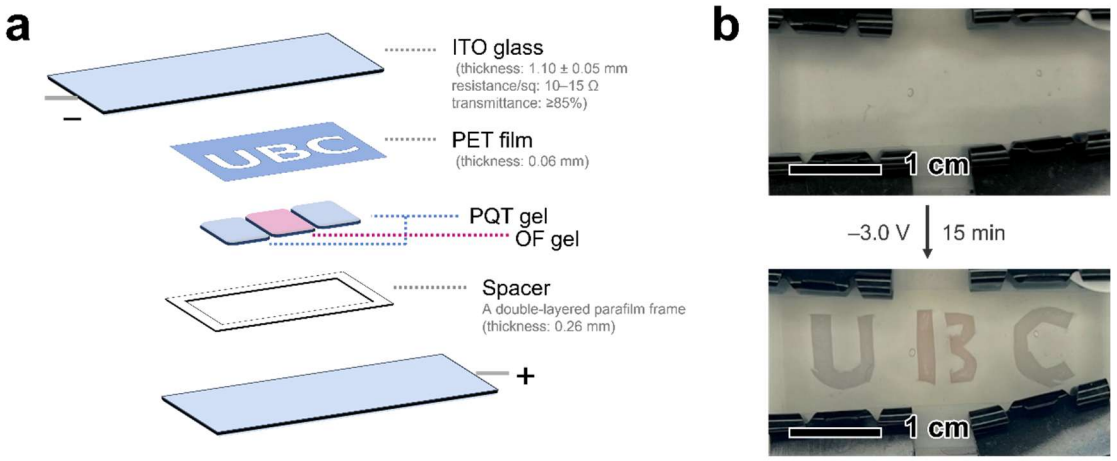

Figure S20. (a) Schematic illustration of the device setup. (b) Photographs of the electrochromic device: the upper image shows the device in the bleached state after 3 days without applying any voltage (after Video S2); the lower image shoes the device after applying –3.0 V for approximately 15 min.

4.4 Sequential electrochromic device

The sequential electrochromic device was fabricated in a sandwich-type assembly, similar to that illustrated in Figure S19. Three double layer parafilm spacers (each spacer area: 10 × 12 mm^2, total thickness: 0.26 mm) were placed between two ITO glass plates to define three adjacent chambers (individual chamber volume: 31 mm^3). The two outer chambers were filled with CNC-DES-**1** and CNC-DES-**3** gels, respectively, while a CNC–viologen photonic film (prepared as described below) was positioned in the central chamber together with a 0.1 M KCl aqueous solution. The device was secured with clips. A PET stencil mask with the "UBC" pattern was attached to one ITO surface to enable spatially controlled coloration of the gels and a film under applied potential. Patterned coloration was recorded by applying a potential of –2.5 to –3.0 V for approximately 20 min, followed by switching the polarity to +3.0 V for approximately 15 min (Video S3). The video was accelerated 15-fold to better visualize the coloration process. Upon reversing the applied potential, the coloration and bleaching process occurred on opposite sides of the device, resulting in bleaching on the originally colored surface and coloration on the opposite surface.

The CNC–viologen photonic film was prepared following our reported procedure.[4] Briefly, CNC-Na^+ (obtained from CelluForce; 6.4 wt%, pH = 6.6) was diluted with deionized water to 3.9 wt% and mixed with *D*-glucose (12.5 wt% relative to CNC). The mixture was sonicated for 2 min, cast into a polystyrene Petri dish (60 mm diameter), and dried under ambient conditions for 1 week to yield an iridescent CNC photonic film. The resulting CNC film was cut into 10 × 10 mm^2 pieces for further use. A 10 × 10 mm^2 piece of CNC film was desulfated by immersion in a NaOH aqueous solution (2.0 M) at 60 °C for 2.5 h, followed by thorough washing with water and methanol, and drying under ambient conditions for 24 h. Covalent attachment of the viologen units was achieved by treating the desulfated CNC film in an HCl aqueous solution (1 mM, pH = 3.0) containing 1-methyl-1′-[3-(trimethoxysilyl)propyl]-4,4′-bipyridinium dichloride (10.0 wt%) at 50 °C for 4 h. The film was then washed with water and methanol, dried, and subsequently immersed in an HCl aqueous solution (1.0 M) at room temperature for 1 h. After further washing with water and methanol and drying under ambient conditions for 24 h, the CNC–viologen photonic film was obtained.

5. In-gel host–guest chemistry

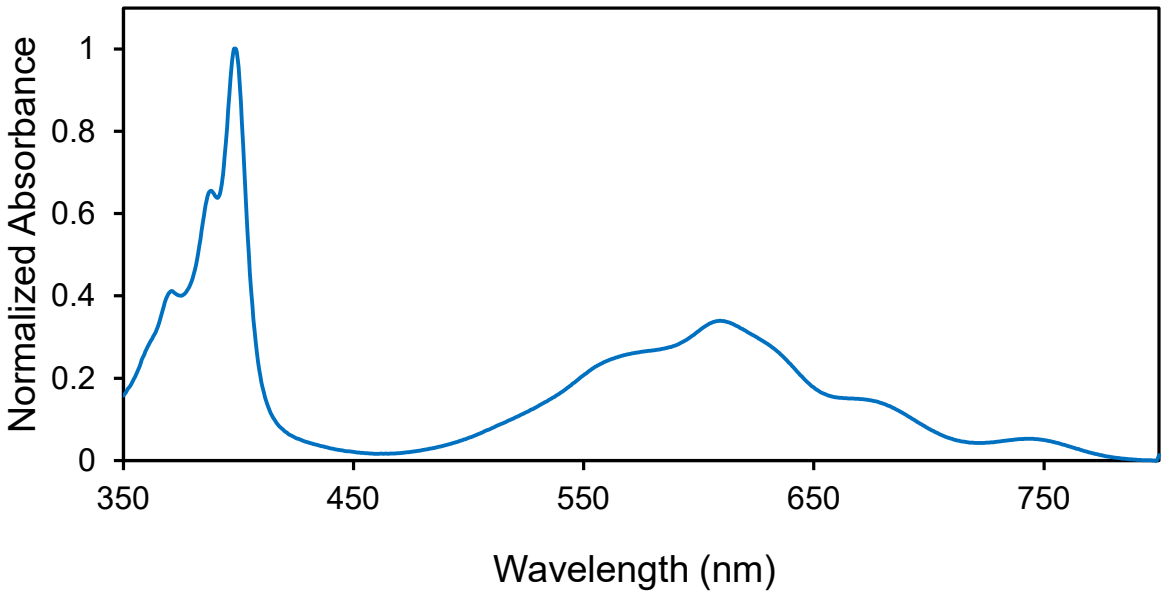

Figure S21. UV-vis spectrum of a CNC–DES–**2** gel produced by photoirradiation (302 nm, 10 min) of CNC–DES–**1**.

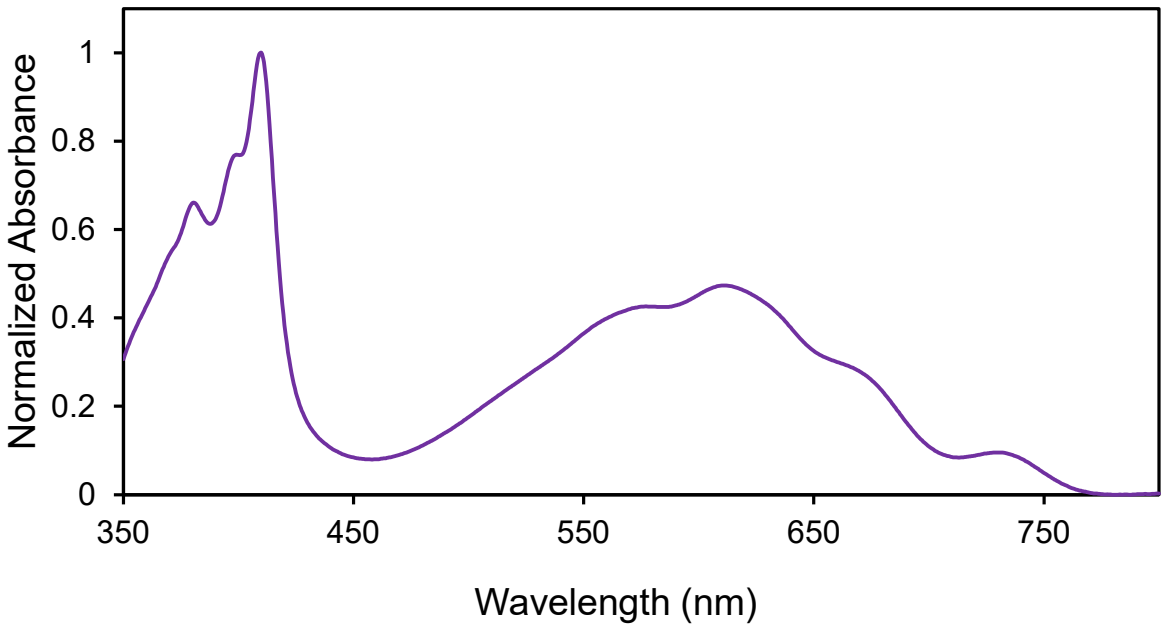

Figure S22. UV-vis spectrum of a CNC–DES–**6** gel produced by photoirradiation (302 nm, 10 min) of CNC–DES–**5**.

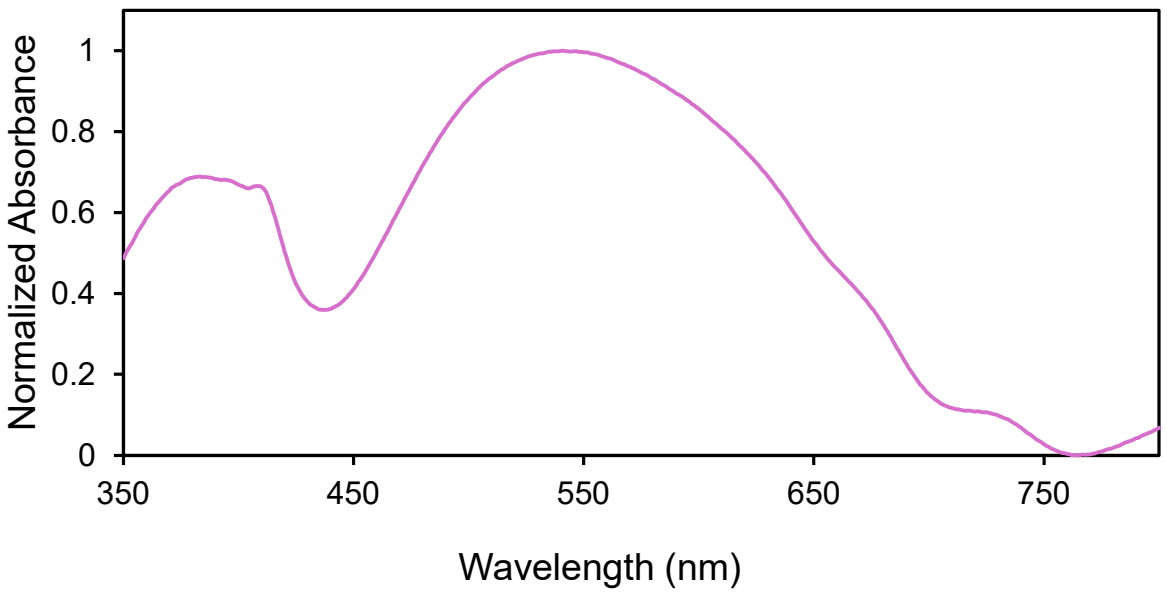

Figure S23. UV-vis spectrum of a CNC–DES–**2/6** gel produced by photoirradiation (302 nm, 10 min) of gel CNC–DES–**1/5**.

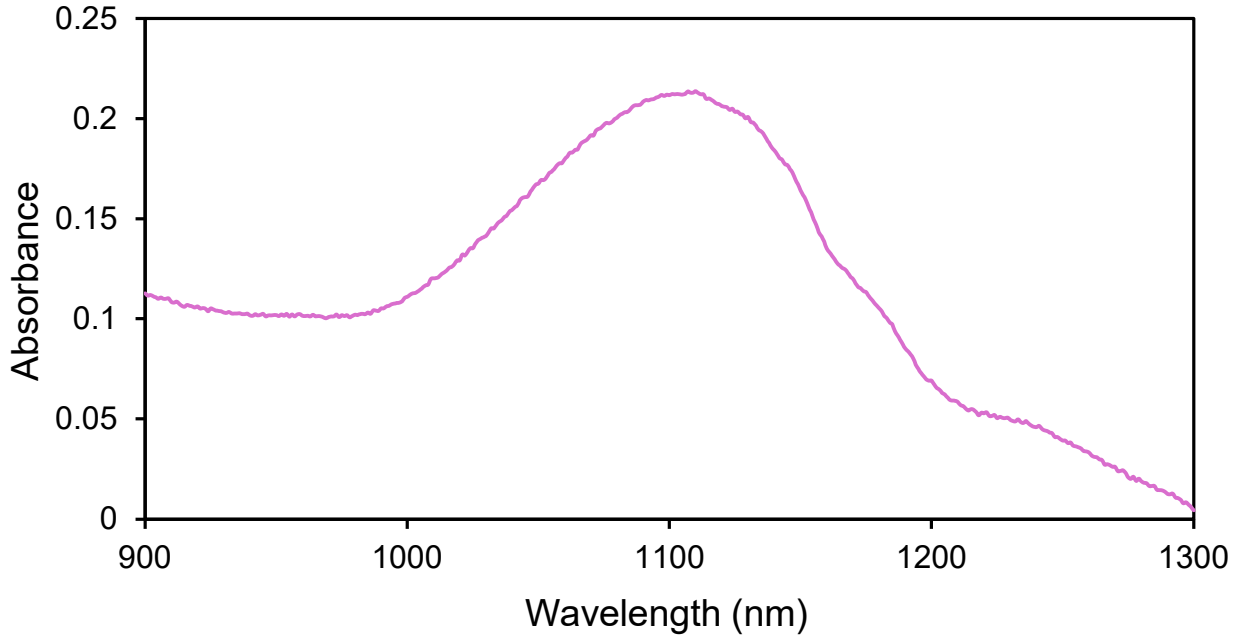

Figure S24. Near-IR region of the UV-vis spectrum of a CNC–DES–**2/6** gel produced by photoirradiation (302 nm, 10 min) of the CNC–DES–**1/5** gel.

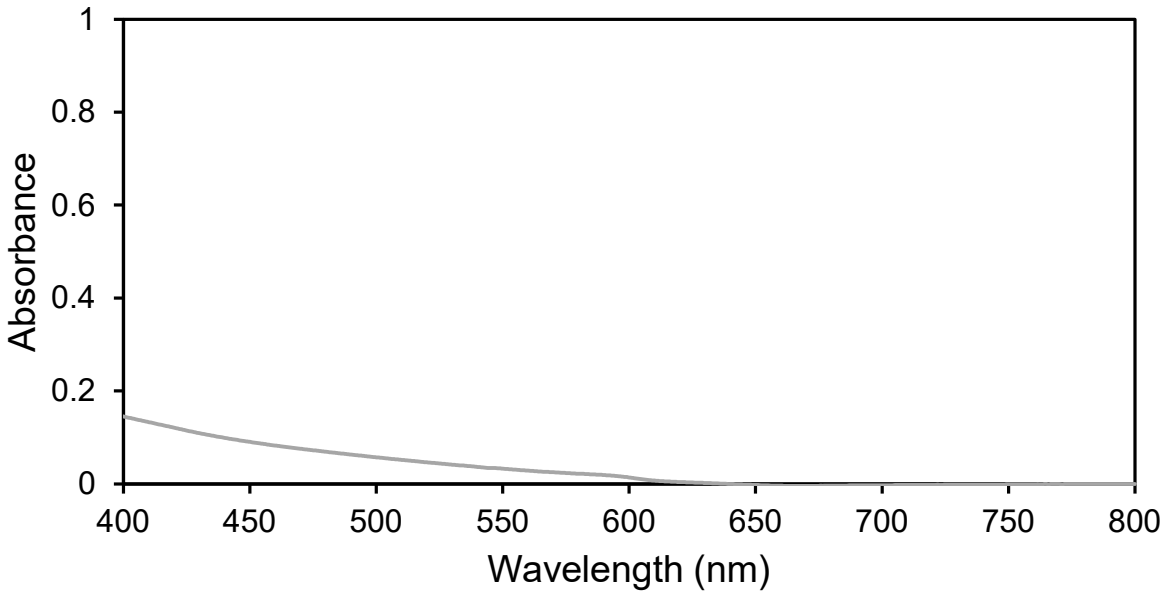

Figure S25. UV-vis spectrum of CNC–DES–**1**/**5** after recovery in the dark (22 h, RT).

6. References

[1] D. Y. Nikumbe, R. G. Pandi, A. Saha, B. Bhatt, S. Bhai, B. Ganguly, S. S. Kumar and R. K. Nagarale, *J. Mater. Chem. A*, 2024, **12**, 25934–25947.

[2] G. Cooke, H. Augier de Cremiers, F. M. A. Duclairoir, M. Gray, P. Vaqueiro, A. V. Powell, G. Rosair and V. M. Rotello, *Tetrahedron Lett.*, 2001, **42**, 5089–5091.

[3] C.-H. Sue, S. Basu, A. C. Fahrenbach, A. K. Shveyd, S. K. Dey, Y. Y. Botros and J. F. Stoddart, *Chem. Sci.*, 2010, **1**, 119–125.

[4] Y. Neagari, M. A. Soto, Y. Zhang, Z. Li, C. A. Michal and M. J. MacLachlan, *Mater. Horiz.,* 2025, **12**, 10184–10193.